where $\epsilon = 1.057$ is the dielectric constant of liquid He. The He depth, d, is determined by measuring the capacitance between the guard ring and the top plate as the cell is filled. Because of capillary action and the meniscus, the uncertainty in d is $\approx \pm 10\%$.

[9]A square lattice, for example, would produce a resonance spectrum significantly different from that we observe. Furthermore, calculations show that the square lattice would have slightly higher energy than the triangular and would be dynamically unstable: G. Meissner, H. Namaizawa, and M. Voss, Phys. Rev. B 13, 1370 (1976); L. Bonsall and A. A. Maradudin, Phys. Rev. B 15, 1959 (1977).

[10]P. M. Platzman and H. Fukuyama, Phys. Rev. B 10, 3150 (1974).

[11]R. W. Hockney and T. R. Brown, J. Phys. C 8, 1813 (1975).

[12]D. J. Thouless, J. Phys. C 11, L189 (1978).

[13]R. C. Gann, S. Chakravarty, and G. V. Chester, to be published.

Phonon-Ripplon Coupling and the Two-Dimensional Electron Solid on a Liquid-Helium Surface

Daniel S. Fisher and B. I. Halperin
Bell Laboratories, Murray Hill, New Jersey 07974, and Harvard University, Cambridge, Massachusetts 02138

and

P. M. Platzman
Bell Laboratories, Murray Hill, New Jersey 07974

(Received 17 January 1979)

We analyze the vibrational modes of a two-dimensional electron solid, coupled to the ripplon modes of a liquid-helium surface, as a function of temperature and external electric pressing field. Resonance observed experimentally by Grimes and Adams are thereby explained.

It has been expected for some time that electrons trapped just above a liquid-helium surface would form a triangular two-dimensional (2D) solid, at sufficiently low temperatures and high densities.[1,2] Experimental demonstration of a phase transition in the trapped-electron system has been obtained by Grimes and Adams[3] as described in the preceding Letter (hereafter referred to as GA). In the present Letter, we analyze the long-wavelength vibrational modes of the electron solid (phonons), taking into account their coupling with ripplons (excitations of the helium surface). The resonances seen in GA are interpreted as arising from the low-lying longitudinal modes, at the discrete vectors $\vec{q}_i$ determined by the geometry.

The vibrational frequency spectrum of the 2D electron solid, in the absence of coupling to ripplons, has been given by several authors.[2] The transverse phonon branch has a linear frequency spectrum at long wavelengths, $\omega_t(q) = c_t q$ ($c_t = 0.245 e^2 n_s^{1/2}/m$ at $T = 0$). Here e, m, and n_s are, respectively, the charge, mass, and areal number density of the electrons. Because of the long-range $1/r$ potential, the longitudinal-mode spectrum of the ideal electron crystal has the form of a 2D plasmon,[4] $\omega_l = (2\pi n e^2 q/m)^{1/2}$. This spectrum is indicated by the dashed curve in Fig. 1.

The spectrum of ripplons on an unperturbed helium surface, ignoring gravity, is given by $\Omega^2(\vec{K}) = \alpha K^3/\rho$, where α and ρ are the surface tension and density of the helium. The ripplons of interest have wave vectors, $\vec{K} = \vec{G}_n + \vec{q}_i$, where $\vec{G}_n$ is a reciprocal-lattice vector of the electron solid. For the triangular lattice, the magnitudes are given by $G_n^2 = nG_1^2$ ($n = 1, 3, 4, 7, 9, \ldots$), where, neglecting possible vacancies and interstitials, $G_1^2 = 8\pi^2 n_s/3^{1/2}$. Since $q_i \ll G_n$, we may, in fact, consider Ω to be independent of $\vec{q}$. The lowest three ripplon frequencies $\Omega_n \equiv \Omega(G_n)$ are indicated by horizontal dashed lines in Fig. 1.

Consider a set of electrons at specified coordinates $\vec{r}(l) = \vec{R}(l) + \vec{u}(l)$ parallel to the surface, where $\vec{u}(l)$ is the horizontal displacement from the lattice position $\vec{R}(l)$. There will be a change in energy due to interaction with ripplons, which we may write as[5]

$$H_I = S^{-1/2}(m\alpha/n_s)^{1/2} \sum_l \sum_{\vec{q}\vec{G}} \xi_{\vec{q}+\vec{G}} V_{\vec{q}+\vec{G}}^0 e^{i\vec{q}\cdot\vec{R}(l)} e^{i(\vec{q}+\vec{G})\cdot\vec{u}(l)}, \quad (1)$$

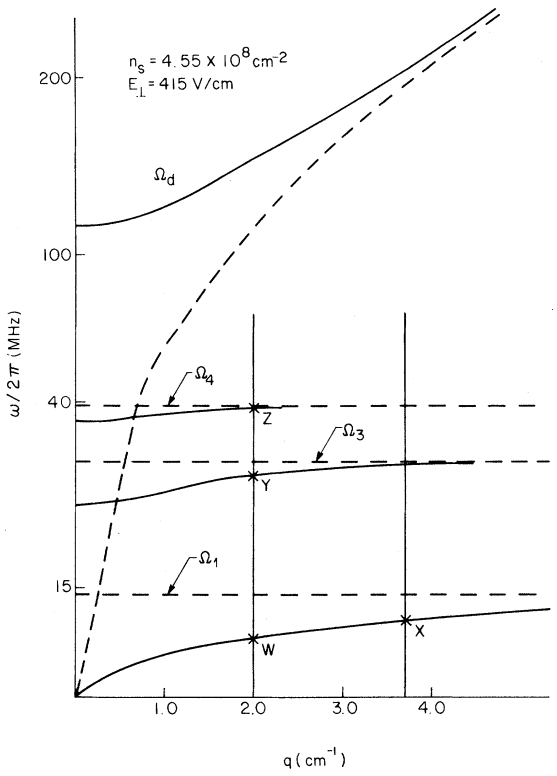

FIG. 1. Schematic of the dispersion relation of the longtitudinal coupled modes (solid curves). The dashed lines show the uncoupled mode spectra and the vertical lines represent the wave vectors excited in the experiment. The resonances are labeled as in Ref. 3.

where $\vec{q}$ is restricted to the first Brillouin zone, $\xi_{\vec{q}+\vec{G}}$ is the Fourier transform of $\xi(\vec{r})$, the vertical displacement of the helium surface at $\vec{r}$, and S is the area. The coefficient $V_K{}^0$ has the form

$$(m\alpha/n_s)^{1/2} V_K{}^0 = eE_\perp + \tfrac{1}{16}(\epsilon - 1)e^2K^2 \ln(\beta/K), \quad (2)$$

where ϵ is the dielectric constant of helium, and $\beta^{-1} \cong 41$ Å is a characteristic distance of the electron from the helium surface. The first term in Eq. (2) arises from interaction with the applied pressing field $E_\perp$, while the second term reflects the variation in the attraction of the image charge due to curvature of the helium surface.

Although we are primarily interested in the behavior of long-wavelength, low-frequency vibrations, it is necessary to take into account the "smearing" of the electronic positions due to high-frequency modes of the electron lattice. To this end, we make a physically motivated approximation. We shall write the displacement $\vec{u}(\vec{l})$ as the sum of a "slow part" $\vec{u}_s$ and a "fast part" $\vec{u}_f$, and we shall replace $e^{i\vec{K}\cdot\vec{u}(\vec{l})}$ in Eq. (1) by

$$\exp(i\vec{K}\cdot\vec{u}_s)\langle\exp(i\vec{K}\cdot\vec{u}_f)\rangle = \exp(i\vec{K}\cdot\vec{u}_s)\exp(-K^2\langle u_f{}^2\rangle/4). \quad (3)$$

The quantity $\langle u_f{}^2\rangle$, which enters the "Debye-Waller factor," is the contribution to the mean-square displacement from the fast modes, and we may write[2]

$$W_1 \equiv \tfrac{1}{4}G_1{}^2\langle u_f{}^2\rangle = \frac{\pi T}{\sqrt{3}mc_t{}^2}\ln\left(\frac{G_1}{q_c}\right) + A(T). \quad (4)$$

Here, q_c is a small-wave-vector cutoff of the "fast modes." The logarithmic dependence on q_c, characteristic of a 2D solid, arises from fluctuations in the transverse phonon modes. The second term in Eq. (4), which contains contributions from short-wavelength fluctuations, scales roughly as T at high T and does to a constant at $T = 0$ due to zero-point fluctuations. If we assume that c_t has its zero-temperature value, then for densities in the range of the experiments ($n_s \cong 4 \times 10^8/\text{cm}^2$), and temperatures near the melting temperature ($T \cong 0.4$°K), we find for q_c in the range 40–500 cm^{-1}, that $0.5 < W_1 < 0.7$.[6] At finite temperatures, the transverse mode may be softened, which would increase W_1.

We can now expand the exponentials $\exp(i\vec{K}\cdot\vec{u}_s)$ in H_I. Terms of zeroth order in $\vec{u}_s$ lead to an equilibrium displacement of the surface, $\langle\xi_{\vec{G}}\rangle \propto V_{\vec{G}}$, where $V_{G_n} = V_{G_n}{}^0\exp(-nW_1) \equiv V_n$ is the reduced coupling constant. This equilibrium displacement is just the "dimple" under the electron position.[7] The next terms in the expansion of $\exp(i\vec{K}\cdot\vec{u}_s)$ lead to an effective interaction Hamiltonian

$$H_I{}^{(2)} = i\sqrt{\alpha}\sum_{\lambda\vec{G}\vec{q}} \xi_{\vec{G}+\vec{q}} Q_{-\vec{q}\lambda} V_{\vec{G}}(\vec{G}+\vec{q})\cdot\vec{e}_{-\vec{q}\lambda} + \tfrac{1}{4}\alpha\sum_{\lambda\vec{G}\vec{q}} V_{\vec{G}}{}^2 G^3[\rho\Omega^2(G)]^{-1} Q_{-\vec{q}\lambda}Q_{\vec{q}\lambda}, \quad (5)$$

where $Q_{\vec{q}\lambda}$ and $\vec{e}_{\vec{q}\lambda}$ are the normal-mode coordinate and polarization vector for a phonon of polarization λ. We have redefined $\xi_{\vec{G}}$ to be the displacement from the dimpled state. The second term in Eq. (5) is the additional restoring force due to the dimples. The total Hamiltonian, free phonon plus free ripplon plus H_I, is quadratic and may be diagonalized in a straightforward manner. {Note that $H_{\text{ripplon}}{}^0 = \sum_{\vec{K}}(\rho/K)[\dot{\xi}_{\vec{K}}{}^2 + \Omega^2(\vec{K})\xi_{\vec{K}}{}^2]$}.

At small q, the secular equation for the eigenfrequencies $\omega(q)$ factors approximately into three

parts. The first two portions describe coupled longitudinal-plasmon–ripplon modes and transverse-phonon–ripplon modes which are shifted from the bare frequencies due to their interactions. These modes, which involve in-plane motion of the electrons, can be excited by spatially dependent ac electric fields *parallel* to the surface. The remaining modes, of which there are at least four at each ripplon frequency, Ω_n, do not involve the phonons and are hence unshifted from the bare ripplon frequencies. [The bare ripplons $\Omega(\vec{G}+\vec{q})$ are at least sixfold degenerate at $q=0$.] One of the unshifted ripplons (at each G_n) involves uniform *vertical* motion of the electrons and, in principle, can be excited by a uniform ac *perpendicular* electric field, as suggested by Monarkha and Shikin.[7] However, an explicit calculation shows that, because of the difficulty in moving electrons vertically, the integrated absorption of these modes is down by factors of order 10^{-9}, proportional to $n_s^{3/2}m/\rho$, compared to the modes involving horizontal electron motion.

We now turn to the coupled longitudinal-phonon–ripplon modes which we believe are the ones observed in GA. The frequency spectra for these modes, indicated by the solid curves in Fig. 1, are obtained from the secular equation,

$$\omega^2-\omega_l^2(q)-\tfrac{1}{2}\sum_{\vec{G}} V_{\vec{G}}^2\,\frac{\omega^2}{\omega^2-\Omega^2(G)}=0. \tag{6}$$

For temperatures near the melting temperature, where $\exp(-2W_1)<0.4$, the sums in Eq. (6) are dominated by the lowest few reciprocal-lattice vectors.

At long wavelength, for the lowest mode, the dimples follow the electrons and the frequency is reduced from the bare longitudinal frequency by a factor $(m/m^*)^{1/2}$, where $m^*\cong m(1+3V_1^2/\Omega_1^2)$ is the effective mass of an electron plus dimple. At shorter wavelengths ($q\gg 10^{-2}$ cm^{-1}), the frequency approaches Ω_1 and is given by

$$\omega^2(q)\cong\Omega_1^2[1+3V_1^2/\omega_l^2]^{-1}. \tag{7}$$

Additional branches of the spectrum lie below each of the higher ripplon frequencies Ω_n. The two lowest ones ($n=3,4$) are given by

$$\omega^2(q)\cong\Omega_n^2-\frac{3V_n^2\Omega_n^2}{\omega_l^2+3V_1^2}. \tag{8}$$

At high frequencies, there is a mode with $\omega^2(q)=\omega_d^2+\omega_l^2$. Here, $\omega_d^2=\frac{1}{2}\sum_{\vec{G}}V_G^2$ is the characteristic frequency of a single electron in a static dimple.

In the presence of an ac electric field of wave vector q, the integrated power absorption by a coupled ripplon-plasmon mode with frequency $\omega(q)$ is

$$\frac{[eE_{\parallel}(q)]^2}{m}\left(1+\tfrac{1}{2}\sum_{\vec{G}}\frac{V_G^2\Omega^2(G)}{[\omega^2(q)-\Omega^2(G)]^2}\right)^{-1}.$$

For the mode with frequency just under the ripplon frequencies Ω_n this will go as V_n^2 and hence be negligible for all but the lowest few modes.

In GA, the electrons are in a cylindrical container of radius $R_0=1.9$ cm, and the standing longitudinal waves excited are expected to be radial. For a boundary condition of no current flow to the walls, the modes will have their wave vectors determined by $J_1(q_iR_0)=0$. The first few values are indicated by the vertical lines in Fig. 1. We interpret three of the resonances seen in GA (W, Y, Z) as the lowest-wave-vector (q_1) resonances, near the ripplon frequencies Ω_1, Ω_3, and Ω_4 and a fourth resonance (X in the figure) as the second spatial mode (q_2) with frequency near Ω_1. Our theory predicts that the resonances lie below the ripplon frequencies Ω_n, and are shifted to lower frequencies with increasing $E_\perp$ and with decreasing temperature (decreasing W_1), and that the shifts are largest for the lower-frequency resonances, all in qualitative agreement with the experiment.

To compare quantitatively with the frequencies given in GA, we chose $n_s=4.55\times10^8$ (within experimental error) and took $\exp(-2W_1)=0.23$. Using a value of ω_t determined from the dispersion relation in Ref. 3 and noting that $E_\perp=2\pi en_s$, Eqs. (7) and (8) yield $W=10.2$, $X=12.3$, $Y=31.4$, and $Z=39.4$ MHz, an essentially perfect fit to the data. We have also fitted the experimental frequencies at other densities and temperatures and achieved similar accuracy with W_1 a smooth function of the dimensionless parameter (see GA) $\Gamma=e^2\sqrt{(\pi n_s)}/T$. At a given density, the variation of the resonant frequencies with $E_\perp$ is in quantitative agreement with experiment. The W_1's in the fit are always a little larger than we estimate, suggesting that a somewhat softer transverse sound velocity is required. Detailed temperature-dependent fitting to the data near the transition will be interesting.

In principle, coupled transverse-phonon–ripplon modes can be experimentally excited by inductive coupling. The spectrum of these modes is obtained from a secular equation of the form of Eq. (6) with ω_t substituted for ω_l. The spectrum is qualitatively similar to that of longitudin-

al modes shown in Fig. 1, but the characteristic wave-vector scale is increased from 1 cm^{-1} to a few hundred inverse centimeters. In particular, at long wavelengths, the lowest transverse mode will have a frequency reduced from the bare phonon frequency $\omega_t(q)$ by the square root of m^*/m.

It should be noted that the calculations in the present paper have assumed small displacements of the electrons. At high driving powers, the electron displacement may be large compared to the lattice constant and the electron velocities may be large compared to the phase velocities of the ripplons. Under such conditions, the electrons will leave the ripplons behind, and excitations may be seen at the bare phonon frequencies $\omega_l(q)$ and $\omega_t(q)$.

We are deeply indebted to Dr. C. C. Grimes for discussions of the emerging experimental data and of the possible theoretical explanations, throughout the course of this investigation. This work has been supported, in part, by the National Science Foundation through Grant No. DMR-77-10210 and a graduate fellowship to one of us (D.S.F.).

[1]R. W. Hockney and T. R. Brown, J. Phys. C 8, 1813 (1975); D. J. Thouless, J. Phys. C 11, L189 (1978); C. C. Grimes, Surf. Sci. 73, 379 (1978).

[2]P. M. Platzman and H. Fukuyama, Phys. Rev. B 10, 3150 (1974); L. A. Bonsall and A. A. Maradudin, Phys. Rev. B 15, 1959 (1977).

[3]C. C. Grimes and G. Adams, preceding Letter [Phys. Rev. Lett. 42, 795 (1979)].

[4]In a real experimental geometry, the plasmon dispersion is modified by the presence of the capacitor plates and is linear at wavelengths large compared to the helium depth [C. C. Grimes and G. Adams, Surf. Sci. 58, 292 (1971)].

[5]P. M. Platzman and G. Beni, Phys. Rev. Lett. 36, 626, 1350(E) (1976); V. B. Shikin and Yu. P. Monarkha, J. Low Temp. Phys. 16, 193 (1974).

[6]For $q < 40$ cm^{-1}, the renormalized shear frequency is less than the linewidths in GA ($\cong 1$ MHz). For $q > 500$ cm^{-1}, the electron motion is primarily in the highest mode with $\omega_l(q) > \omega_d \cong 6 \times 10^8$ sec^{-1}. On physical grounds, we expect the cutoff q_c to lie between these limits.

[7]Yu. P. Monarkha and V. B. Shikin, Zh. Eksp. Teor. Fiz. 68, 1423 (1975) [Sov. Phys. JETP 41, 710 (1976)].

Occupied Surface-State Bands in *sp* Gaps of Au(112), Au(110), and Au(100) Faces

P. Heimann and H. Miosga
Sektion Physik der Universität München, D-8000 München 22, Federal Republic of Germany

and

H. Neddermeyer
Institut für Experimentalphysik der Ruhr-Universität, D-4630 Bochum, Federal Republic of Germany

(Received 27 November 1978)

We have identified occupied surface-state bands from angle-resolved photoelectron energy distribution curves of Au(112), Au(100), and Au(110), which are located in *sp* gaps of the projected bulk band structure. An approximate criterion for their possible experimental existence is given.

It is now experimentally well established that the (111) faces of the noble metals exhibit occupied surface states in the center of the two-dimensional Brillouin zone (2D BZ).[1-6] Dispersion of the surface-state bands has been determined by angle-resolved photoelectron spectroscopy showing that these surface states exist in the gap at point L of the bulk band structure. The energetical minimum of these surface-state bands occurs in the [111] direction, around which a fairly symmetrical distribution in $\vec{k}$ space is observed.

Recently Williams *et al.* investigated a (211) face of Cu,[7] which consists of three-atom terraces of (111) orientation separated by one-atom steps of (100) orientation $\{(S)\text{-}[3(111)\times(100)]$ structure$\}$. They found surface states pointing into the [111] direction of the (211)-oriented single crystal from which they concluded that these surface states are associated with the (111) terraces of Cu.

In the present Letter we report on photoemission results from a (211) face of Au, which cannot be explained by the interpretation given in Ref. 7. Instead, the occurrence of surface states on the (211) face of Au appears as a general property of the *sp* gap around the L point of the three-

